V1 Projection Zone Signals in Human Macular Degeneration Depend on Task, not Stimulus

Yoichiro Masuda[1,2], Serge O. Dumoulin[1], Satoshi Nakadomari[2] and Brian A. Wandell[1]

[1]Psychology, Stanford University, Stanford, CA 94305, USA and [2]Ophthalmology, Jikei University, School of Medicine, Tokyo, 105-8461 Japan

We used functional magnetic resonance imaging to assess abnormal cortical signals in humans with juvenile macular degeneration (JMD). These signals have been interpreted as indicating large-scale cortical reorganization. Subjects viewed a stimulus passively or performed a task; the task was either related or unrelated to the stimulus. During passive viewing, or while performing tasks unrelated to the stimulus, there were large unresponsive V1 regions. These regions included the foveal projection zone, and we refer to them as the lesion projection zone (LPZ). In 3 JMD subjects, we observed highly significant responses in the LPZ while they performed stimulus-related judgments. In control subjects, where we presented the stimulus only within the peripheral visual field, there was no V1 response in the foveal projection zone in any condition. The difference between JMD and control responses can be explained by hypotheses that have very different implications for V1 reorganization. In controls retinal afferents carry signals indicating the presence of a uniform (zero-contrast) region of the visual field. Deletion of retinal input may 1) spur the formation of new cortical pathways that carry task-dependent signals (reorganization), or 2) unmask preexisting task-dependent cortical signals that ordinarily are suppressed by the deleted signals (no reorganization).

Keywords: feed-back, fMRI, human, plasticity, retinal degeneration, visual cortex

Introduction

During visual development abnormal retinal signals can influence cortical circuit development, and specifically visual field maps. In human visual cortex, for example, congenital retinal disease transforms the visual field map in human primary visual cortex (Morland et al. 2001; Baseler et al. 2002).

In adult primary visual cortex, reports differ on how the cortical responses change following retinal damage. Using functional magnetic resonance imaging (fMRI) in a subject with age-related macular degeneration, Sunness et al. (2004) report no significant responses in a large region of primary visual cortex deprived of retinal input. On the other hand, Baker et al. (2005) describe measurements in macular degeneration subjects that show significant fMRI responses in the V1 lesion projection zone (LPZ) of the diseased retina. They find these responses in some, but not all, subjects (Dilks et al. 2006). They acknowledge that little is known about the neural origin of these responses, and they describe several alternative hypotheses about how these V1 responses might be generated (Baker et al. 2005).

Here, we investigate the nature of these responses using fMRI measurements in primary visual cortex of juvenile

macular degeneration (JMD) subjects. These subjects were presented with a variety of visual stimuli and 3 types of tasks. During passive viewing, or when performing judgments unrelated to the stimulus, the V1-LPZ produced essentially no response. When JMD subjects engaged in a stimulus-related judgment (one-back task [OBT]), highly significant responses were present in V1 regions located within the LPZ (3 out of 4 subjects). Hence, visual stimulation alone did not produce a response in the LPZ; a stimulus-related task was necessary. No responses were measured in nonstimulated regions of control subjects, even when a stimulus-related task was used.

There are several possible explanations for these results. The explanation we favor supposes that in control subjects there is a balance between the retinal input signal indicating zero-contrast and the cortico-cortical signals during the OBT. According to this model, in the JMD subjects the balance between geniculo-cortical and cortico-cortical signals in the LPZ is disturbed. The absence of a geniculo-cortical signal representing the zero stimulus contrast unmasks the task-dependent cortico-cortical signals and produces a response in the LPZ. Thus, the model explains the increased activity in the JMD subjects not by the spread of a feed-forward signal, but rather from the deletion of this signal.

Materials and Methods

Data were acquired at 3 sites: Kanagawa Rehabilitation Hospital, National Institute of Information and Communications Technology (NICT), Japan and Stanford University, USA. There were slight differences in the methodology but the results from the 3 sites are in excellent agreement. When the methods differ we specify the settings. Data from the 3 sites were analyzed at Stanford University using identical data analysis techniques.

Subjects

We report measurements from 7 subjects; 4 subjects with JMD (JMD1–4; specifics see Table 1) and 3 control subjects with normal vision (C1–3). The JMD subjects were diagnosed with 1 of 2 types of JMD: cone-rod dystrophy, or Stargardt disease. The JMD subjects had neither additional eye-related diseases nor any other neurological problems. All JMD subjects used their dominant eye for the experiments. We estimated the dominant eye using a visual alignment task (Porac and Coren 1976). In all subjects, the foveal retina or macular retina is damaged creating a central scotoma. In the absence of a functional fovea the JMD subjects developed a preferred retinal locus (PRL) in the periphery to accomplish visual task ordinarily performed with foveal fixation.

A visual representation of the PRL and the visual field regions with an absolute scotoma are shown in Figure 1. Absolute scotomas were defined as regions in visual space where the subjects failed to detect the highest contrast and largest size stimulus that standard Goldmann perimetry can supply. We suspect that these JMD subjects have additional regions surrounding these scotomas with decreased visual

Table 1
JMD subjects' profiles

Patient	Gender	Diagnosis	Time course (years)			Lesion size (degrees)		Log MAR BCVA		Scanned eye
			Onset	Duration	Age	Right	Left	Right	Left	
JMD1	Female	Cone-rod dystrophy	18	13	31	50 × 40	50 × 45	+1.30	+1.16	Left
JMD2	Male	Stargardt disease	9	13	22	30 × 30	30 × 30	+1.0	+1.1	Left
JMD3	Male	Cone-rod dystrophy	28	10	38	50 × 45	60 × 50	+1.7	+1.7	Right
JMD4	Male	Stargardt disease	41	16	57	8 × 5	8 × 5	+0.90	+0.90	Right

Note: Lesion size; horizontal × vertical, Log MAR BCVA; Logarithm of the minimum angle of resolution best-corrected visual acuity.

sensitivity (relative scotomas) especially between their absolute scotoma and PRL locations.

Cone-rod dystrophy and Stargardt disease are both inherited progressive diseases. They have similar symptoms but result from different mutations (Glazer and Dryja 2002; Hamel 2007).

JMD 1 and 3 were diagnosed with cone-rod dystrophy, an inherited progressive disease where lipofuscins-like materials (waste deposits) accumulate predominantly in the foveal retinal pigment epithelium (RPE). As a result cone photoreceptors deteriorate first, followed by rod photoreceptors. The symptoms of cone-rod dystrophy are decreased visual acuity, color vision defects, photoaversion, and decreased sensitivity in the central visual field; these symptoms are followed by progressive loss in peripheral vision and night blindness. The diagnosis of cone-rod dystrophy is based on clinical history, fundus examination and decline of full-field electroretinogram (Scullica and Falsini 2001; Hamel 2007).

JMD2 and 4 were diagnosed with Stargardt disease, also an inherited progressive disease. Similarly to cone-rod dystrophy, lipofuscins-like materials accumulate in the RPE and as a result, photoreceptors degenerate. The symptoms include decreased visual acuity, decreased sensitivity in the central visual field. The diagnosis of Stargardt disease is based on clinical history, fundus examination, fluorescein angiogram and electroretinograms (Glazer and Dryja 2002). Unlike cone-rod dystrophy, the full-field electroretinogram are normal at an early stage (Scullica and Falsini 2001), but at later stages it is difficult to distinguish cone-rod dystrophy and Stargardt disease.

JMD1 (female, age 31) was diagnosed with cone-rod dystrophy at age 18. During the MR measurements, she viewed the stimulus with her left eye and the right eye was covered with a patch. She has a bilateral absolute central scotoma spanning approximately 50 × 45° diameter in the measured eye (Fig. 1A and Supplemental Fig. 1). JMD1 has 2 PRLs in the left eye but mainly uses a primary PRL located in the left lower visual field about 15° from the fovea (Fig. 1A). Her visual field was measured using standard Goldmann perimetry. The location of the PRL and absolute scotoma edge were confirmed with a Rodenstock (Ottoburnn, Germany) scanning laser ophthalmoscope (SLO). In the MR experiments she fixated using her primary PRL. An infrared-video eye-monitoring system (ST-661; NAC Image Technology, Tokyo, Japan) was used to observe fixation stability (for an example dataset see Supplemental Fig. 2). Her fixation stability was statistically indistinguishable for the different viewing conditions.

JMD2 (male, age 22) was diagnosed with Stargardt disease at age 9. The subject viewed the stimuli with his left eye and a patch covered the right eye. His absolute central scotoma is about 30 × 30° in diameter (Fig. 1B and Supplemental Fig. 1) in both eyes. He uses a PRL on the left lower visual field (Fig. 1B and Supplemental Fig. 1); his visual field was estimated using custom built stimuli (see Behavioral perimetry in Materials and Methods).

JMD3 (male, age 38) was diagnosed with cone-rod dystrophy at age 28. Measurements were made using his right eye and an eye patch covered the left eye. He has an absolute central scotoma of about 50 × 45° in diameter in the measured eye (Fig. 1C and Supplemental Fig. 1). He fixated using a PRL on the lower visual field. His visual field was measured with standard Goldmann perimetry and the PRL location and absolute scotoma edge were verified relative to the absolute scotoma using an SLO. His fixation was monitored by an infrared-video eye-monitoring system (ST-661; NAC Image Technology, Tokyo, Japan). His fixation stability was statistically indistinguishable for the different viewing conditions.
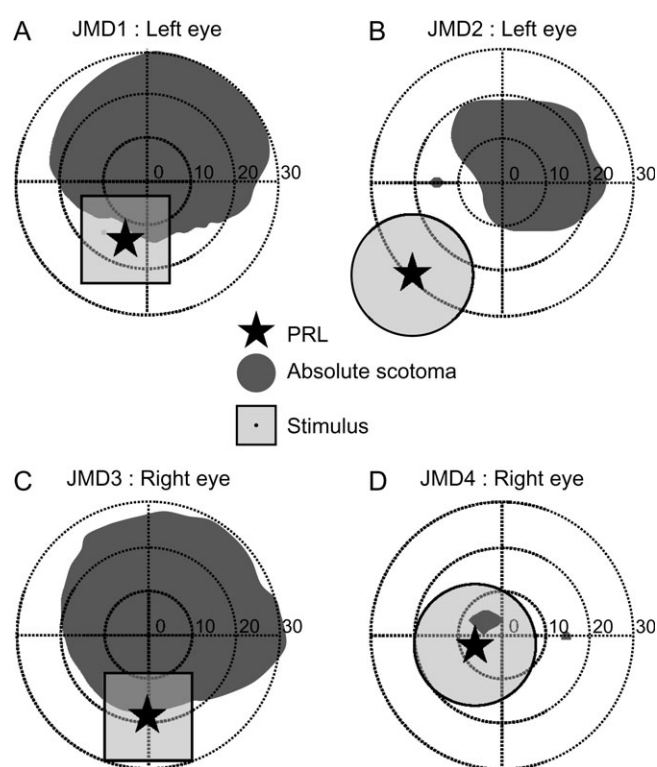
Figure 1. A schematic diagram of the subjects' visual fields and stimulus position. (A–D) The visual field and stimulus position is shown for the measured eye in JMD1–JMD4, respectively. Dark gray regions represent absolute scotomas; the transparent light gray regions show the visual field location of the stimulus. The star indicates the subjects' PRL. In JMD1, 3 (A, C) the foveal position was estimated by monitoring the visual axis during visual field measurement, and in JMD2, 4 (B, D), the foveal position was estimated by the location of the physiological blind spots. Note that relative scotomas usually exist between the PRL and the absolute scotoma region. Units are degrees of visual angle.

JMD4 (male, age 57) was diagnosed with Stargardt disease at age 41. Measurements were made using his right eye and a patch covered the left eye. He has an absolute scotoma about 8 × 5° in diameter in both eyes (Fig. 1D and Supplemental Fig. 1). We estimated the location of this absolute scotoma relative to the position of his anatomical blind spot. Our estimates place his absolute scotoma slightly off the central fovea. However, the absolute scotoma is surrounded by a relative scotoma as estimated with a multifocal electroretinogram, and his foveal function is deteriorated to such a degree that he developed a PRL. He fixated using a PRL on the left lower visual field in his right eye; his visual field was estimated using custom build stimuli (see Behavioral perimetry in Materials and Methods).

C1/2/3 (all male; ages 29-35) maintained fixation on a right upper point relative to the visual stimulus; consequently the stimuli fell on a part of the retina corresponding to the location of the PRL of JMD1. In essence, we simulate the viewing conditions of JMD1 by placing the

stimulus at an identical retinal location. No other stimulus modifications were made. We refer to the retinal location where the stimulus was presented as the simulated PRL, and the foveal representation where no stimulus was present as the simulated LPZ (sLPZ). Like JMD1 the control subjects used their left eye only and a patch covered the right eye.

The data from subjects JMD1, JMD3, and C1–3 were acquired at NICT; additional JMD3 data were acquired at Kanagawa Rehabilitation Hospital; subjects JMD2, and JMD4 were measured at Stanford University. All procedures adhered to protocols based upon the world medical association declaration of Helsinki ethical principles for medical research involving human subjects, approved by the ethical committees of Kanagawa Rehabilitation Hospital, NICT, and Stanford University. All subjects provided written informed consent to participate in the project.

Behavioral Perimetry
The visual fields of JMD1, 3 were measured by Goldmann perimetry. We used kinetic targets and defined the absolute scotoma as the region they could not detect the highest contrast and largest size stimulus (size V, 1.6° diameter). For subjects where no Goldmann perimetry data were available (JMD2, 4), we estimated the visual field deficit using custom software in the Matlab programming environment using the PsychToolbox (Brainard 1997; Pelli 1997). The methods were comparable to standard Humphrey perimetry procedures and the settings aimed to detect absolute scotomas only. The subjects were asked to indicate whether they perceived a brief stimulus presentation of 0.05 s, while maintaining fixation with their PRL. The stimulus consisted of a circular dot (maximum luminance) placed on a gray background (the gray background intensity was the 0.5 log unit lower than the target dot). The dot size was 1.6° diameter, comparable with the standard Goldmann perimetry size V.

MR Stimuli
The visual stimuli consisted of reversing checkerboards, drifting contrast patterns, scrambled, and intact faces (Table 2). The stimulus subtended 20 or 28° diameter (Japan and Stanford University, respectively). JMD subjects viewed a fixation point at the center of the stimulus using their PRL; they maintained PRL-fixation throughout the experiment. In control subjects the fixation point was displaced so that the stimuli fell on a retinal location that corresponded to PRL of the JMD1 subject.

The stimuli were shown in a block-design where alternating blocks showed the stimuli or baseline periods of uniform gray field (mean luminance). The duration of each block was 15 or 12 s (Japan and Stanford University, respectively). Except for the reversing checkerboard pattern, images were presented every 750 or 1000 ms during each block (Japan and Stanford University, respectively). Each run contained 6 or 10 stimulus blocks (Stanford University and Japan, respectively).

Three different task conditions and several different stimuli were used; these are summarized in Table 2. In one task condition, the subjects viewed stimuli passively and did not perform a task. In the 2nd task condition the subjects performed a fixation task, consisting of detecting a color change of the fixation-dot. For some JMD subjects (JMD1 and JMD3) this task was beyond their visual capabilities. In the 3rd task condition, the subjects performed a task consisting of reporting 2 consecutive repetitions of the same stimulus, known as the OBT.

Two different stimuli were used during the OBT scans: drifting contrast patterns or faces. In drifting contrast patterns, the motion direction is changing in consecutive presentations and the subjects reported 2 consecutive repetitions of the same motion direction. When viewing faces subjects reported whether the face was repeated. Some of the JMD subjects viewed the same stimuli during passive measurements, as well. Subjects performed well during the tasks; during the fixation task and OBT correct response rates were over 95%.

At Kanagawa Rehabilitation Hospital and NICT, Japan, the stimuli were presented using a D-ILA projector (DLA-G150, Victor Company of Japan, Japan) and publicly provided software (Visual Basic 6.0, Direct X 7.0., Microsoft). At Stanford the stimuli were generated in the Matlab programming environment using the PsychToolbox (Brainard 1997; Pelli 1997) on a Macintosh G4 Powerbook and presented using an LCD projector (LT158, NEC, Santa Clara, CA). Subjects viewed the display through a mirror mounted above the head.

Scanning Procedure

Japanese Data
The MRI data of JMD1 and JMD3 and the corresponding controls (C1–3) were acquired on a 3-T Siemens Trio scanner (Erlangen, Germany), NICT. Additional data were acquired for JMD3 on a 1.5-T Siemens Vision Plus scanner (Erlangen), Kanagawa Rehabilitation Hospital. fMRI images (T_2^*-weighted blood oxygenation level–dependent [BOLD] responses) were collected parallel to the AC–PC line through the occipital lobes using a single-shot gradient echo planer imaging sequence (3-T: 37 planes; time repetition/time echo [TR/TE], 3000/36 ms; flip angle, 90°; voxel size, $2 \times 2 \times 2$ mm; field of view [FOV], 192 mm; 1.5-T: 24 planes; TR/TE, 3000/66 ms; flip angle, 90°; voxel size, $3 \times 3 \times 3$ mm; FOV, 192 mm).

Stanford Data
The MRI data of JMD2 and JMD4 were acquired on a 3-T General Electric scanner (Milwaukee, WI). fMRI images (T_2^*-weighted BOLD responses) were collected orthogonal to the calcarine sulcus using a 2-dimensional spiral sequence (TR/TE, 1500/30 ms; flip angle, 55°; effective voxel resolution, $2.5 \times 2.5 \times 3$ mm) (Glover and Lai 1998; Glover 1999). Eye movements of JMD2 and 4 were not measured during the experiment. However, in this study, fixation accuracy is not crucial for the result, because the LPZ stays fixed on the cortex whichever way the eye is pointed.

A high-resolution anatomical T_1-weighted MRI volume scan of the entire head was also obtained for each subject (voxel size, $1 \times 1 \times 1$ mm).

Data Analysis and Visualization
Data were analyzed using the mrVista software (Stanford, http://white.stanford.edu/software) (Wandell et al. 2000). The first 10 time frames in each functional run were discarded due to start-up magnetization transients in the data. The remaining time frames were corrected for motion (Nestares and Heeger 2000). No spatial smoothing was performed. The fMRI signals were converted to percent signal change by dividing and subtracting each voxel's time series by the time-series mean. Baseline drifts were removed from the time series by high-pass temporal filtering.

We calculated the phase-specified coherence of each fMRI series at the fundamental stimulus frequency to measure the strength of the BOLD responses (Bandettini et al. 1993; Logothetis and Wandell 2004; Liu and Wandell 2005). The phase-specified coherence (C) is defined as:

$$C = \frac{A_0}{\sqrt{\sum A_f^2}} \cos(\theta_0 - \varphi)$$

where A_f are the amplitude of each Fourier component (f), and A_0 and θ_0 are the amplitude and phase of the signal at that stimulation frequency, and φ is the hemodynamic response delay. The phase-specified

---

Table 2
The table indicates which experiments were performed in each subject

Subjects	Drifting contrast patterns			Intact faces		Reversing checkerboards	Scrambled faces
	Passive viewing	Fixation task	OBT	Fixation task	OBT	Passive viewing	Passive viewing
JMD1		X	●	X	●	○	○
JMD2	○	○	●			○	
JMD3	○	X	●	X			
JMD4		○	○	○	○		

Note: Certain combination of stimuli and task yielded stimulus-synchronized responses in the LPZ (solid circles), whereas others did not (open circles). The X indicates that the subjects were not able to perform the fixation task and thus no data were obtained. This table shows that stimulus-synchronized responses in the LPZ were observed in JMD1–3 only during the OBT and independent of the stimulus.

coherence values range between −1 and 1; positive values reflect stronger responses to the stimulus presentations, whereas negative values reflect stronger responses to the mean-luminance presentations. We estimate the phase from the fMRI time course in the cortical PRL representation; this is the location where the most reliable activation is found. We refer to responses in this phase and at the stimulus alternation frequency as stimulus-synchronized.

Gray matter was segmented from the high-resolution anatomical volume for each subject, rendered in 3 dimensions close to the white matter boundary and unfolded using publicly available software (Teo et al. 1997; Wandell et al. 2000). Activations were visualized on the unfolded representation of the white–gray matter boundary.

Results

No stimulus-Synchronized Responses in the LPZ during Passive Viewing

The activation elicited during passive viewing of scrambled faces is shown on an inflated cortical surface of the posterior right hemisphere of JMD1 and a control subject (C1) (Fig. 2). The activations shown by the pseudocolors all exceed an absolute phase-specified coherence level of 0.30. We show the data on the inflated right hemisphere because JMD1 and all of the other JMD subjects have PRLs that include the left visual field (Fig. 1). Therefore, we expect the PRL projection zone (PRL-PZ) to be present in the right hemisphere.

In both JMD1 and C1 there is significant activation in the right upper anterior bank of calcarine sulcus. This cortical location is fully consistent with the PRL-PZ during passive viewing, which is in the left lower visual field (Fig. 1A).

The average time series for 1 stimulus cycle are shown in the panels on the left and right. Each time-series measures the response in a circular (3 mm radius) region of interest (ROI); these are indicated by the white circles on the inflated brain. The ROI centers are placed every 5 mm along the shortest line across the cortical surface from the PRL-PZ to the occipital pole. The occipital pole usually overlaps with the foveal projection zone and receives input from the lesioned retina.

There is a large region, spanning more than 1.5 cm and including the occipital pole, which is nonresponsive or only weakly responsive. We define the LPZ as this nonresponsive region extending from outside the PRL-PZ to the occipital pole. The data do not permit us to identify a sharp border between the PRL-PZ and the LPZ. In part, this may be because the surround region of the PRL-PZ can receive input from incompletely affected retina. We indicate the transition between the PRL-PZ and LPZ by the blurred region in the colored line beside the average time series (Fig. 2).

In JMD1 during passive viewing, there is a strong stimulus-synchronized response in the PRL-PZ. In the region adjacent to the PRL-PZ there are small modulations, but these modulations are much smaller than those in the PRL-PZ and quite unlike the activity in normal stimulus-driven cortex. These small modulations at the stimulus alternation frequency may be driven by retinal signals that have been affected by incomplete retinal degeneration. There is a significant response in the occipital pole in counterphase to the stimulus phase (negative BOLD) (Fig. 2, left panel bottom graphs). This response profile is not restricted to passive viewing of scrambled faces; responses elicited during passive viewing of reversing checkerboards are very similar.

In C1 (and C2/3) the simulated PRL projects to the simulated PRL-PZ, and the region between simulated PRL-PZ
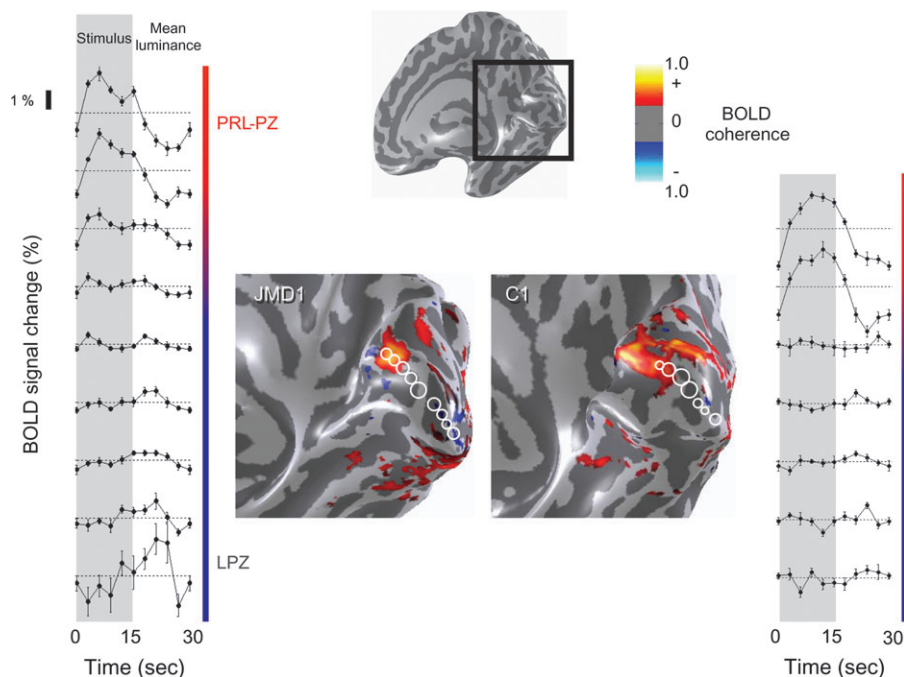
Figure 2. Passive viewing stimuli elicit stimulus-synchronized response in the PRL-PZ but not the LPZ. The response elicited during the passive viewing of scrambled faces is shown on an inflated cortical surface of the right hemisphere. The black box shows the position of the expanded region showing the phase-specified coherence map in JMD1 and C1. All data overlaid on the inflated brain exceed an absolute phase-specified coherence level of 0.30. The graphs show the average response during 1 stimulus cycle in a set of ROIs. The ROI positions (3-mm-radius circles) are shown on the cortical surface, spanning the shortest line connecting the PRL-PZ to the occipital pole. In JMD1, no stimulus-synchronized response is observed in the LPZ; in some regions near the occipital pole the response to the mean luminance exceeds the response to the stimulus (negative BOLD; left bottom graphs). In C1, the response patterns qualitatively resemble those of JMD1. The average single time curves show no stimulus-synchronized activity in the sLPZ.

and occipital pole is the sLPZ. During passive viewing the responses in C1 are similar to those in JMD1, and there is very little or no negative BOLD response in the occipital pole.

Stimulus-Synchronized Responses in the LPZ during OBT

Next we measured these subjects while viewing face stimuli and performing an OBT. Stimulus-synchronized responses in JMD1 were strongest in the PRL-PZ; weaker but significant responses extended beyond the PRL-PZ spreading into the LPZ (Fig. 3, left panel bottom graphs). Recall that during passive fixation these same regions failed to respond or responded in counterphase to the stimulus (Fig. 2, left panel bottom graphs).

The large increase in the spatial extent of the responsive region within V1 during the OBT was not observed in the control subject, C1 (Fig. 3, right panel). Although the absolute size of the response is slightly larger; there are still no significant stimulus-synchronized responses in the control subject's sLPZ.

There is a strong increase in the responses in ventral regions normally occupied by hV4, VO-1, VO-2, and the FFA during the OBT with the face stimuli (Fig. 3) compared with the passive viewing with scrambled faces (Fig. 2).

These differences could be due to the task difference, or it could be due to the stimulus difference (faces vs. scrambled faces). In subsequent experiments with other JMD subjects, we show that it is due to the task difference.

Stimulus-Synchronized Responses in the LPZ Depend on Task not Stimulus

Face stimuli are not essential to reveal this difference between the JMD and control subjects. In a separate experiment we presented drifting contrast patterns with OBT (same or different motion direction). Despite the stimulus difference, the spatial distribution of responses in JMD1 was very similar (Fig. 5B; solid black curve, circles).

In other JMD subjects we made measurements using the same stimulus (drifting gratings) in both passive viewing and during the OBT (Fig. 4). In JMD2 and 3, there are zero or negative responses in the LPZ during passive viewing (JMD2, 3) or when performing a fixation-dot task (JMD2). When the subjects performed a stimulus-related OBT, a stimulus-synchronized response was present in the LPZ. Hence, the increased activation in the LPZ elicited during the OBT is not specific to stimulus type (Table 2).

In JMD4 and the control subjects there were no responses in the LPZ either with or without the OBT. Hence, JMD subjects can differ.

Quantification of the V1 Spatial Response Profile

We measured the spatial profile of phase-specified coherence as a function of distance from the PRL-PZ to the occipital pole in JMD1 and in 3 controls (Fig. 5). The PRL-PZ location was estimated by locating the small region that responds during passive viewing; the occipital pole was defined on anatomical grounds. We selected 3-mm radius circular ROIs on the cortical surface. The distance between ROIs was 5 mm. We then plotted the mean phase-specified coherence in each ROI as a function of the distance of the ROI from the PRL-PZ to the occipital pole. In JMD1 and C1, the ROIs are the same as Figures 2 and 3. The absolute distance between the PRL-PZ and the occipital pole differs among subjects, therefore we plot the normalized distance.

In control subjects (Fig. 5A), the decline in phase-specified coherence as one measures from the simulated PRL-PZ toward the occipital pole, is similar for all stimuli and tasks.
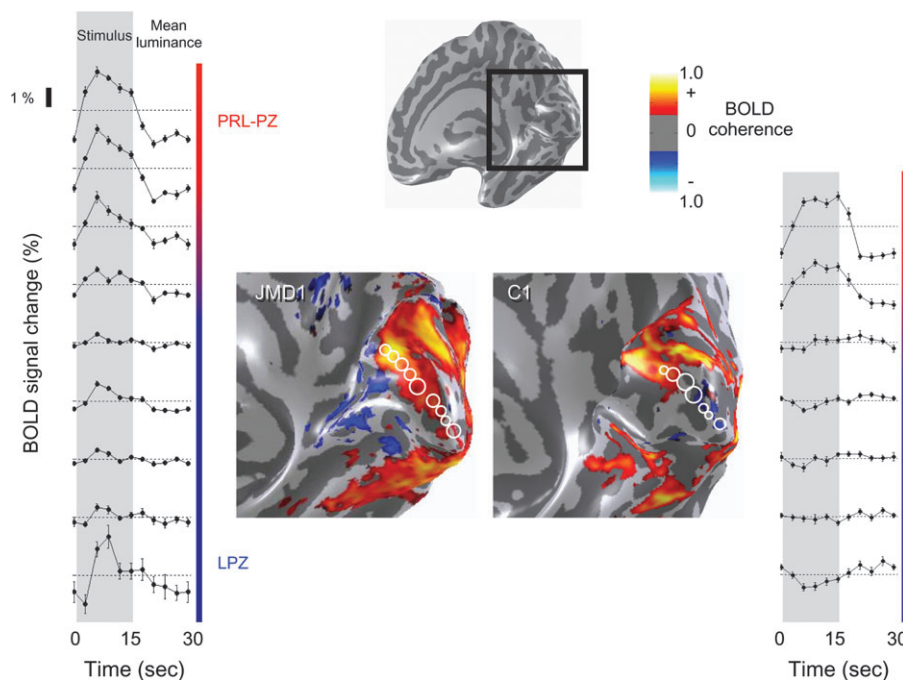

Figure 3. During the OBT, stimulus-synchronized responses are present in the LPZ of JMD1 but not in C1. The data are shown in an identical format as figure 2. The left panel shows stimulus-synchronized responses that extended beyond the PRL-PZ into the LPZ of JMD1. Note the occipital pole that previously responded preferentially to the mean-luminance presentations (Fig. 2, left bottom graphs), now responds in phase with the stimulus (Fig. 3, left bottom panels). In C1 this response was not observed, although some regions responded stronger to the mean-luminance presentations. In both subjects, increased responses in ventral cortex can be observed.
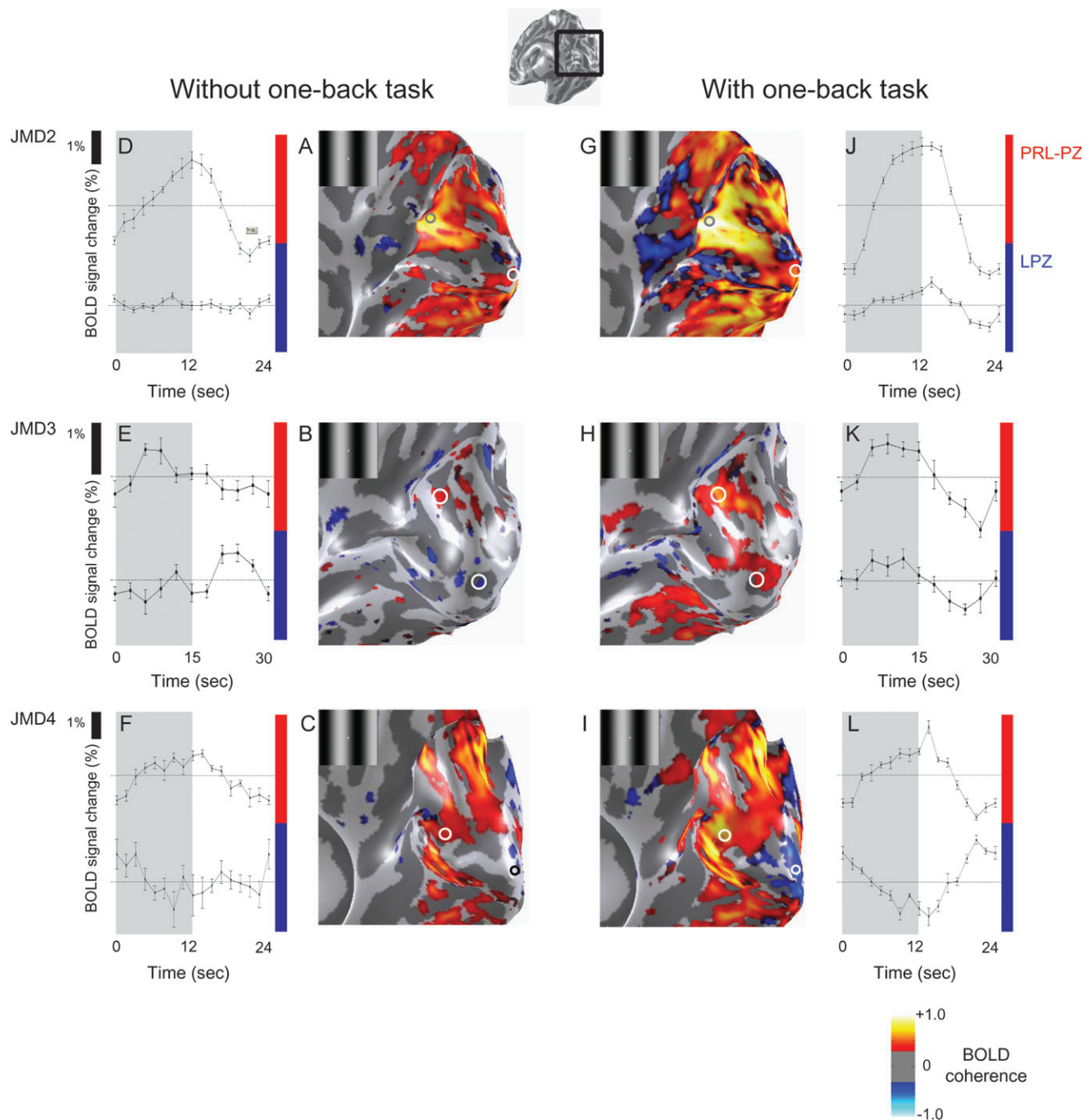
Figure 4. Viewing the stimuli while performing the OBT elicits a stimulus-synchronized response in the LPZ in JMD2, 3 but not in JMD4. We compare the activation pattern elicited by passive viewing (JMD2, 3) or stimulus unrelated judgments (JMD4) (left panels) and OBT (right panels) of the drifting contrast pattern (insets). The panels from the 3 rows are JMD2, 3, 4, respectively. (*A–C*) The phase-specified coherence map. (*D–F*) The average time course during 1 stimulus cycle in the PRL-PZ (top) and the LPZ (bottom). Stimulus-synchronized responses are present in the PRL-PZ and negative or weak responses are present in the occipital pole. (*G–L*) Stimulus-synchronized responses while performing the OBT, are shown in an identical format to figure (*A–F*). In JMD2 and 3, a stimulus-synchronized response is elicited in the PRL-PZ and the LPZ, even though there should not be any input from the lesioned retina. In JMD4, a stimulus-synchronized response in the LPZ is not observed, although some regions responded stronger to the mean-luminance presentations (*L*). Ventral, dorsal, and lateral occipital responses increase during the OBT condition.

In JMD1 the decline in phase-specified coherence depends on the task (Fig. 5*B*). In the passive viewing condition the responses fall near the distribution for the controls (Fig. 5*B*, dotted lines and shaded region). During the OBT, however, the responses in JMD1 spread over a larger cortical distance and remain positive all the way to the occipital pole (Fig. 5*B*, solid lines). As we measure adjacent to the PRL-PZ, the responses during passive viewing are similar or lower than the normal range, whereas the responses during the OBT are higher than the normal range. Near the occipital pole regions with negative BOLD in passive viewing respond in phase with the stimulus (positive BOLD) during the OBT; this transformation occurs for both types of stimuli, faces, and drifting contrast patterns. Thus, in JMD1 changing to OBT from passive
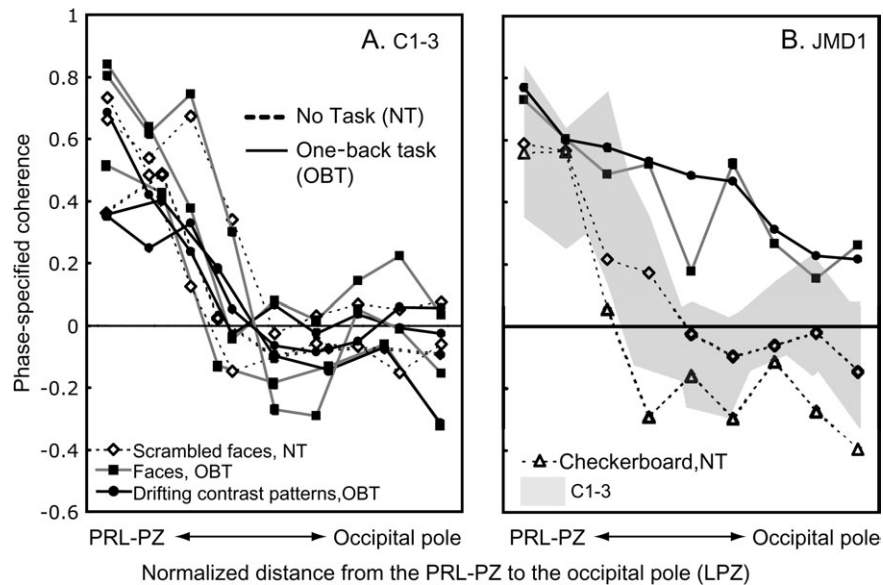
Figure 5. The spatial profile of phase-specified coherence in controls (C1–3) and JMD1. The spatial profile of phase-specified coherence is plotted as a function of distance from the PRL-PZ to occipital pole (A) in 3 controls, and (B) the comparison of JMD1 and controls (gray shadow). The 3-mm-radius circle ROIs are selected on the cortical surface from the PRL-PZ to the occipital pole chosen along the shortest line connecting the 2 locations. The distance between the ROIs is 5 mm. The distance between the PRL-PZ and the occipital pole is different among the subjects, therefore we show the normalized distance. A solid line indicates the phase-specified coherence from viewing stimuli with the OBT, whereas dotted lines indicate the phase-specified coherence elicited by passive viewing of the stimuli (no task; NT) or viewing the stimuli with the fixation task (fixation task; FT in Fig. 6). In the control subjects, the phase-specified coherence decreases with increasing distance from the simulated PRL-PZ. This decrease of the phase-specified coherence is similar for all viewing conditions (A). For JMD1 (B), when passively viewing the stimuli, at increasing distance from the PRL-PZ into the occipital pole (LPZ) the coherence levels decrease to negative or close to negative values (B, dotted lines). The OBT elicits strong positive coherence levels around the occipital pole (LPZ) (B, solid line) as compared with passive viewing (B, dotted lines) and the control subject (B, gray shadow). Almost all error bars are hidden within symbols.

viewing significantly alters the phase-specified coherence responses within the LPZ.

We also measured the spatial profile of phase-specified coherence in JMD2–4 subjects (Fig. 6). In JMD2 and JMD3 the phase-specified coherence pattern is similar to that observed in JMD1. In passive fixation, there remain large regions of silent V1 (Fig. 6A,B, dashed lines). During the OBT, the spatial distribution of the response increases in amplitude and extends to the occipital pole (Fig. 6A,B, solid lines). Thus, the OBT changes the phase-specified coherence in the occipital pole from near-zero or negative to positive in 3 JMD subjects. The change in the coherence is 1) independent of the specific stimulus, and 2) an additional 0.2-0.4 increase in the coherence level. In JMD4, diagnosed at the oldest age of our subjects, with the smallest scotoma and some residual foveal function, there is no effect of the task; the cortical response is similar in all tasks and stimuli (Fig. 6C).

Discussion

During passive viewing, or performing unrelated judgments (fixation task), we found large silent zones in primary visual cortex of JMD subjects. But, we measured stimulus-synchronized responses in the LPZ in 3 out of 4 of these subjects when they engaged in the OBT (Figs 2–6, Table 2). The relationship between task and LPZ activity was observed using a range of stimuli. Therefore, we conclude that the observed stimulus-synchronized responses in the LPZ are not stimulus-driven, but rather they are driven by the stimulus-related task.

The data demonstrate a significant difference in neural signals between JMD1–3 and controls. Even when controls perform a stimulus-related task, we do not observe a cortical response in the sLPZ.

Our results provide a unifying framework for resolving the conflicting observations in noncongenital human macular degeneration subjects. Some of these previous studies (Baker et al. 2005), but not others (Sunness et al. 2004), described stimulus-synchronized activation in the LPZ (Table 3). This is consistent with our observations in 3 out of 4 JMD subjects during the OBT. We note that the subjects in Baker et al. actively performed a OBT, whereas the subject of Sunness et al. did not.

An important unanswered question concerns the neural basis for the difference between the controls and JMD subjects. We consider several possible explanations.

Eye Movements

We don't believe differences in eye-movement patterns explain our results. First, fixation accuracy is not crucial for the result, because the LPZ stays fixed on the cortex whichever way the eye is pointed. Second, we recorded eye-movements in 2 JMD subjects and found no significant difference in their eye-movements with or without performing a OBT (Supplemental Fig. 2).

Incomplete Scotoma Characterization

It is possible that there are a few spared pathways from the fovea to the LPZ. Such pathways might carry a signal that is too weak to be detected under passive viewing, but that is amplified and detectable during the OBT. However, for JMD1–3, the stimulus did not extend into the central fovea (Fig. 1). Hence, spared foveal pathways would not be stimulated and could not produce the observed stimulus-synchronized response in the LPZ. We note that the controls have intact foveal pathways, and no response was observed in these subjects (Figs 2, 3, 5A).
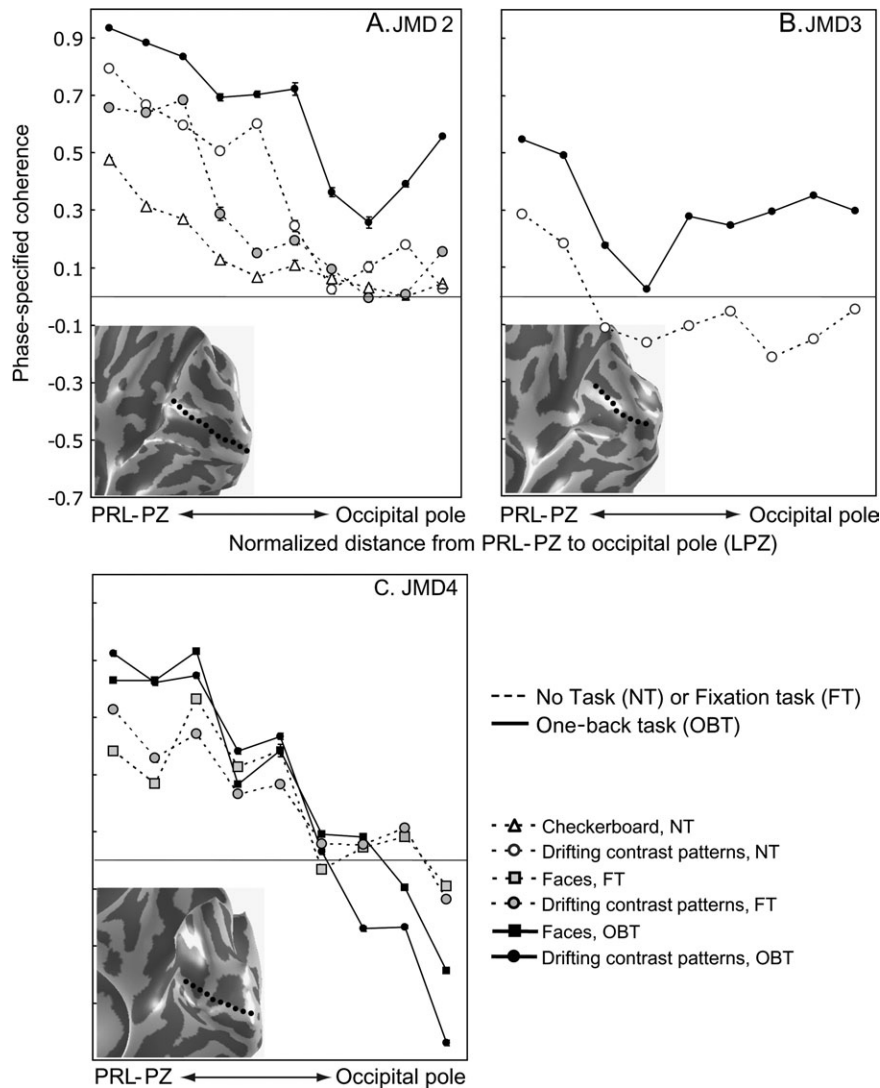
Figure 6. The spatial profile of phase-specified coherence in JMD2–4. The spatial profile of phase-specified coherence as a function of distance from the PRL-PZ to the occipital pole in 3 JMD subjects (*A–C*). The data are shown in an identical format as Figure 5. The insets in the graphs show the corresponding cortical surface and the shortest line from the PRL-PZ to the occipital pole (dotted line). The PRL-PZ always yields a positive phase-specified coherence level. When passively viewing the stimuli or performing stimulus unrelated judgments, at increasing distance from the PRL-PZ into the occipital pole the coherence levels decrease to negative or close to negative values. The OBT elicits strong positive coherence levels around the occipital pole except for JMD4 as compared with passive viewing or stimulus unrelated judgments and the control subjects (Fig. 5*A*). In JMD4, the decrease from the PRL-PZ of the phase-specified coherence is similar for all viewing conditions (*C*).

Lateral Spread of Feed-forward Signals

Baker et al. (2005) considered the hypothesis that the stimulus-synchronized responses in the LPZ reflect large-scale re-organization of visual stimulus processing in adult human subjects. They discussed 3 possible mechanisms underlying the LPZ responses. One mechanism entailed feed-back signals whereas the other 2 were feed-forward reorganizations of the signal that extend the spatial distribution of retinal signals into the LPZ at the level of the LGN or V1. These 2 proposals imply cortical reorganization of visual processing in adults similar to reports of cortical reorganization in human congenital retinal dystrophy (Morland et al. 2001; Baseler et al. 2002), human early blindness (Sadato et al. 1996, 2002; Cohen et al. 1997) and animal studies (Kaas et al. 1990; Chino et al. 1992; Gilbert and Wiesel 1992; Darian-Smith and Gilbert 1995; Gilbert 1998; Kaas 2002; Giannikopoulos and Eysel 2006; but see Murakami et al. 1997; Horton and Hocking 1998; Smirnakis et al. 2005).

The hypothesis that task-dependent responses reflect new connections from the LGN to the LPZ, or amplification of feed-forward signals spreading laterally within V1, seems unlikely. As Baker et al. (2005) point out, the large size (several centimeters) of the LPZ in the JMD subjects means that the horizontal connections would have to spread much farther than the longest horizontal connections reported in primate V1 (6–8 mm) (Gilbert et al. 1996; Angelucci et al. 2002). It is possible that these horizontal connections are extended by a poly-synaptic chain or "axonal sprouting" (Darian-Smith and Gilbert 1994). But the hypothesis seems unlike because even in that case, feed-forward responses should be present regardless of the task.

It is possible that weak feed-forward lateral connections are formed subsequent to the lesion. These pathways may be insufficient to produce a response to the visual stimulus during passive viewing; they only become detectable when amplified

| Diagnosis age at the experiment, gender	Location, size of the absolute scotoma (horizontal × vertical, degrees)	Stimulus-synchronized responses in the LPZ	Onset (age)	Course (years)	PRL	OBT experiment	Author
JMD (cone–rod dystrophy) Age 56, male	B-fovea 20 × 20 < (B)	Yes	Late of 30's	16<	Yes	Yes	Baker et al. 2005
JMD Age 50, male	B-fovea 34 × 34 < (B)	Yes	11	39	Yes	Yes	Baker et al. 2005
AMD Age 60, female	B-perifovea	No	57	3	No	No	Sunness et al. 2004
JMD1 (cone–rod dystrophy) Age 31, female	B-fovea 50 × 40(R) 50 × 45(L)	Yes	18	13	Yes	Yes	Masuda et al.
JMD2 (Stargardt disease) Age 22, male	B-fovea 30 × 30(R) 30 × 30(L)	Yes	9	13	Yes	Yes	Masuda et al.
JMD3 (cone–rod dystrophy) Age 38, male	B-fovea 50 × 45(R) 60 × 50(L)	Yes	28	10	Yes	Yes	Masuda et al.
JMD4 (Stargardt disease) Age 57, male,	B-fovea 8 × 5(R) 8 × 5(L)	No	41	16	Yes	Yes	Masuda et al.

Note: B; both eyes, R; right eye, L; left eye.

by a powerful task demand (Huk and Heeger 2000). In this case, the task would affect responses in both the PRL-PZ and LPZ; consistent with that prediction we do observe an increase of the signal strength in the PRL-PZ for all JMD subjects (Figs 5 and 6) even when using identical stimuli (Fig. 6). But task-dependent response increases in the PRL-PZ differ from the response changes in the LPZ; specifically, in the LPZ the OBT changes the fMRI signals from negative to positive in 2 subjects (JMD1, JMD3). Negative BOLD responses are usually inter-preted as neuronal deactivation (Shmuel et al. 2006; Pasley et al. 2007), and a transformation from negative to positive BOLD response is inconsistent with an amplification of an existing signal. Rather, the task-dependent response changes are consis-tent with an additive change in neuronal activity in the LPZ.

Unmasking Feed-back Signals

The possibility we favor is based on feed-back from extrastriate visual cortex into the LPZ (Fig. 7). Specifically, we propose that stimulus-synchronized responses in the LPZ are driven by cortico-cortical signals elicited by the demands of the OBT. In macaques, these feed-back signals from extrastriate cortex (e.g. MT) can influence V1 regions that do not themselves provide input to those extrastriate cortical units (Zeki and Shipp 1988) and spread far enough to modulate the LPZ (MT to V1 projection field is ~27° (Angelucci et al. 2002; Harrison et al. 2007). This hypothesis is consistent with the very large task-dependent increase in the extrastriate cortex during the OBT (Figs 3 and 4). The task-dependent increase in extrastriate responses, particularly on the ventral surface, is quite clear in Figures 2–4. In addition, several studies show that cortico-cortical signals can modulate the fMRI signal in early visual cortex. These cortico-cortical signals could carry signals related to attention (Brefczynski and DeYoe 1999; Gandhi et al. 1999; Martinez et al. 1999; Somers et al. 1999), visual imagery (Klein et al. 2000, 2004; Slotnick et al. 2005), or task-related low-level visual processing.

The hypothesis also is consistent with the absence of V1 responses in controls. In these subjects V1 receives a zero-contrast geniculo-cortical signal that indicates the blank screen; we presume this response nulls the cortico-cortical task-dependent signals (Fig. 7B). In JMD subjects, the missing geniculo-cortical input to the LPZ makes the feed-back signals the dominant source of neuronal activity (Fig. 7D).
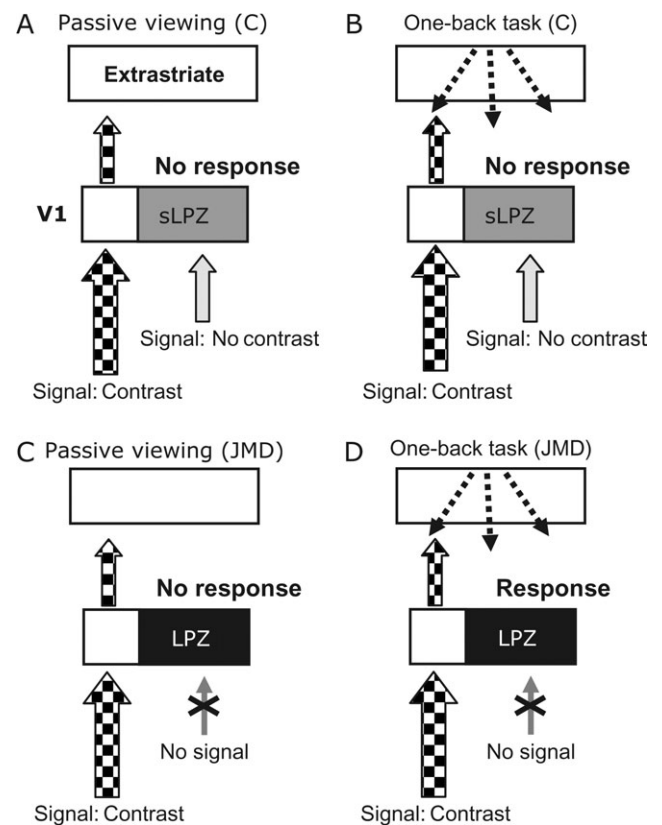
Figure 7. Responses in the LPZ may result from an imbalance in geniculo-cortical and cortico-cortical projections. (A) Control subjects, passive viewing: the contrast pattern in the periphery elicits a V1 and extrastriate response. The zero-contrast signal from the foveal region elicits no response. (B) Control subjects, OBT: The OBT elicits a task-dependent V1 cortico-cortical feed-back signal (dashed arrows). There is also a zero-contrast geniculo-cortical signal in the sLPZ. The combination of these 2 signals produces no activation in the LPZ. (C, D) In JMD subjects, there is no feed-forward signal from damaged retina. In passive viewing, no V1 signal is expected. But during the OBT cortico-cortical signals are not met by a corresponding zero-contrast geniculo-cortical signal. Consequently, feed-back signals are unmasked in V1 (and elsewhere), producing a stimulus-synchronized activation in the LPZ.

Finally, this hypothesis is consistent with the response heterogeneity of the JMD subjects (Dilks et al. 2006; Masuda et al. 2006). First, some JMD subjects may still have some remaining retino-cortical signals due to a nonabsolute (relative)

scotoma or partially overlapping binocular scotomas. Second, smaller absolute scotomas may not produce a large imbalance because this balance could be regulated at the coarse level of the feed-back (e.g., JMD4). Third, the output layers of V1 are binocular, so that in monocular JMD subjects the feed-forward and feed-back signals would be balanced similar to healthy cortex (Dilks et al. 2006). Fourth, passive viewing does not enforce an attentional state, so that some differences can arise from the uncontrolled passive viewing condition. Hence, small differences in the nature of the scotomas and the subjects' attentional states—differences that cannot be easily measured—may have significant impacts on the relative balance between the signals converging within V1 and introduce heterogeneity into the population measurements.

Cellular Basis of the Task-Dependent Signals

Many experiments in cat and monkey, spanning more than a decade, report substantial reorganization in primary visual cortex (Kaas et al. 1990; Chino et al. 1992; Gilbert and Wiesel 1992; Darian-Smith and Gilbert 1995; Gilbert 1998; Kaas 2002; Giannikopoulos and Eysel 2006); a few do not (Horton and Hocking 1998; Smirnakis et al. 2005).

There are important differences between the cellular measurements showing map reorganization and the fMRI measurements reported here and by others. First, the reports in animal models are generally done under anesthesia, and thus cannot be attributed to the task demands as in our case. Second, the experiments in cat and monkey demonstrate a reduction of the LPZ by no more than 6–8 mm. The reduction of the LPZ described here and by Baker et al. (2005) is on the order of several centimeters. Hence, the fMRI measurements we describe may not represent the same cellular mechanism described in anesthetized animals.

The data we present do not exclude the possibility that there is some cortical reorganization. It is conceivable that cortical reorganization occurred at the border of the LPZ, either shifting this border or locally changing the neurons receptive field size (Darian-Smith and Gilbert 1995; Gilbert et al. 1996; Gilbert 1998; Kaas 2002; but see Smirnakis et al. 2005). It is clear, however, that after many years of macular degeneration, human visual cortex contains regions spanning several centimeters in width that are unresponsive or very weakly responsive to the stimulus. In this sense, our observations represent a powerful limit on the scale of adult cortical plasticity in visual cortex.

Definition of Cortical Reorganization

Visual stimuli combined with an appropriate task can activate the deprived visual foveal cortex (LPZ); this does not occur in control subjects. Baker et al. interpreted these abnormal cortical signals as evidence for "large-scale reorganization" (Baker et al. 2005). Large-scale reorganization implies large changes in neuronal architecture, for example, synaptic gain or axonal connections. We choose not to call these abnormal signals "reorganization" because deletion of existing cortical circuitry can explain these signals without assuming any changes in the neuronal architecture. In general, we note that abnormal signals per se do not imply the presence of cortical re-organization. Invoking reorganization as the cause of abnormal signals should include specific evidence and modeling.

Summary

We observed stimulus-synchronized responses in the LPZ of 3 JMD subjects. These responses are not driven principally by retinal contrast, but by a stimulus-judgment task. Although several explanations of the LPZ responses are possible, we propose that they are driven by cortico-cortical signals elicited by the task demands. On this hypothesis, the stimulus-synchronized responses in the LPZ of the JMD subjects reflect an imbalance between geniculo-cortical and cortico-cortical projections to the LPZ created by the deletion of retinal input signals.

Supplementary Material

Supplementary material can be found at: http://www.cercor.oxfordjournals.org/.

Notes

Address correspondence to Yoichiro Masuda, Wandell Laboratory, Jordan Hall, Building 420, Stanford University, Stanford, CA 94305, USA. Email: massuuu@gmail.com.

References

Angelucci A, Levitt JB, Walton EJ, Hupe JM, Bullier J, Lund JS. 2002. Circuits for local and global signal integration in primary visual cortex. J Neurosci. 22:8633–8646.

Baker CI, Peli E, Knouf N, Kanwisher NG. 2005. Reorganization of visual processing in macular degeneration. J Neurosci. 25:614–618.

Bandettini PA, Jesmanowicz A, Wong EC, Hyde JS. 1993. Processing strategies for time-course data sets in functional MRI of the human brain. Magn Reson Med. 30:161–173.

Baseler HA, Brewer AA, Sharpe LT, Morland AB, Jagle H, Wandell BA. 2002. Reorganization of human cortical maps caused by inherited photoreceptor abnormalities. Nat Neurosci. 5:364–370.

Brainard DH. 1997. The psychophysics toolbox. Spat Vis. 10:433–436.

Brefczynski JA, DeYoe EA. 1999. A physiological correlate of the 'spotlight' of visual attention. Nat Neurosci. 2:370–374.

Chino YM, Kaas JH, Smith EL, 3rd, Langston AL, Cheng H. 1992. Rapid reorganization of cortical maps in adult cats following restricted deafferentation in retina. Vision Res. 32:789–796.

Cohen LG, Celnik P, Pascual-Leone A, Corwell B, Falz L, Dambrosia J, Honda M, Sadato N, Gerloff C, Catala MD, et al. 1997. Functional relevance of cross-modal plasticity in blind humans. Nature. 389:180–183.

Darian-Smith C, Gilbert CD. 1994. Axonal sprouting accompanies functional reorganization in adult cat striate cortex. Nature. 368:737–740.

Darian-Smith C, Gilbert CD. 1995. Topographic reorganization in the striate cortex of the adult cat and monkey is cortically mediated. J Neurosci. 15:1631–1647.

Dilks DD, Baker CI, Peli E, Kanwisher NG. 2006. Reorganization of cortical visual processing: further evidence from individuals with macular degeneration. Atlanta (GA): Society for Neuroscience.

Gandhi SP, Heeger DJ, Boynton GM. 1999. Spatial attention affects brain activity in human primary visual cortex. Proc Natl Acad Sci USA. 96:3314–3319.

Giannikopoulos DV, Eysel UT. 2006. Dynamics and specificity of cortical map reorganization after retinal lesions. Proc Natl Acad Sci USA. 103:10805–10810.

Gilbert CD. 1998. Adult cortical dynamics. Physiol Rev. 78:467–485.

Gilbert CD, Das A, Ito M, Kapadia M, Westheimer G. 1996. Spatial integration and cortical dynamics. Proc Natl Acad Sci USA. 93:615–622.

Gilbert CD, Wiesel TN. 1992. Receptive field dynamics in adult primary visual cortex. Nature. 356:150–152.

Glazer LC, Dryja TP. 2002. Understanding the etiology of Stargardt's disease. Ophthalmol Clin North Am. 15:93–100viii.

Glover GH. 1999. Simple analytic spiral K-space algorithm. Magn Reson Med. 42:412–415.

Glover GH, Lai S. 1998. Self-navigated spiral fMRI: interleaved versus single-shot. Magn Reson Med. 39:361–368.

Hamel CP. 2007. Cone rod dystrophies. Orphanet J Rare Dis. 2:7.

Harrison LM, Stephan KE, Rees G, Friston KJ. 2007. Extra-classical receptive field effects measured in striate cortex with fMRI. Neuroimage. 34:1199–1208.

Horton JC, Hocking DR. 1998. Monocular core zones and binocular border strips in primate striate cortex revealed by the contrasting effects of enucleation, eyelid suture, and retinal laser lesions on cytochrome oxidase activity. J Neurosci. 18:5433–5455.

Huk AC, Heeger DJ. 2000. Task-related modulation of visual cortex. J Neurophysiol. 83:3525–3536.

Kaas JH. 2002. Sensory loss and cortical reorganization in mature primates. Prog Brain Res. 138:167–176.

Kaas JH, Krubitzer LA, Chino YM, Langston AL, Polley EH, Blair N. 1990. Reorganization of retinotopic cortical maps in adult mammals after lesions of the retina. Science. 248:229–231.

Klein I, Dubois J, Mangin JF, Kherif F, Flandin G, Poline JB, Denis M, Kosslyn SM, Le Bihan D. 2004. Retinotopic organization of visual mental images as revealed by functional magnetic resonance imaging. Brain Res Cogn Brain Res. 22:26–31.

Klein I, Paradis AL, Poline JB, Kosslyn SM, Le Bihan D. 2000. Transient activity in the human calcarine cortex during visual-mental imagery: an event-related fMRI study. J Cogn Neurosci. 12(Suppl. 2):15–23.

Liu J, Wandell BA. 2005. Specializations for chromatic and temporal signals in human visual cortex. J Neurosci. 25:3459–3468.

Logothetis NK, Wandell BA. 2004. Interpreting the BOLD signal. Annu Rev Physiol. 66:735–769.

Martinez A, Anllo-Vento L, Sereno MI, Frank LR, Buxton RB, Dubowitz DJ, Wong EC, Hinrichs H, Heinze HJ, Hillyard SA. 1999. Involvement of striate and extrastriate visual cortical areas in spatial attention. Nat Neurosci. 2:364–369.

Masuda Y, Nakadomari S, Asakawa K, Dumoulin SO, Liu J, Cheung SH, Ben-Shachar M, Kitahara K, Wandell BA. 2006. Lack of cortical reorganization in macular degeneration patients. Atlanta (GA): Society for Neuroscience.

Morland AB, Baseler HA, Hoffmann MB, Sharpe LT, Wandell BA. 2001. Abnormal retinotopic representations in human visual cortex revealed by fMRI. Acta Psychol (Amst). 107:229–247.

Murakami I, Komatsu H, Kinoshita M. 1997. Perceptual filling-in at the scotoma following a monocular retinal lesion in the monkey. Vis Neurosci. 14:89–101.

Nestares O, Heeger DJ. 2000. Robust multiresolution alignment of MRI brain volumes. Magn Reson Med. 43:705–715.

Pasley BN, Inglis BA, Freeman RD. 2007. Analysis of oxygen metabolism implies a neural origin for the negative BOLD response in human visual cortex. Neuroimage. 36:269–276.

Pelli DG. 1997. The VideoToolbox software for visual psychophysics: transforming numbers into movies. Spat Vis. 10:437–442.

Porac C, Coren S. 1976. The dominant eye. Psychol Bull. 83:880–897.

Sadato N, Okada T, Honda M, Yonekura Y. 2002. Critical period for cross-modal plasticity in blind humans: a functional MRI study. Neuroimage. 16:389–400.

Sadato N, Pascual-Leone A, Grafman J, Ibanez V, Deiber MP, Dold G, Hallett M. 1996. Activation of the primary visual cortex by Braille reading in blind subjects. Nature. 380:526–528.

Scullica L, Falsini B. 2001. Diagnosis and classification of macular degenerations: an approach based on retinal function testing. Doc Ophthalmol. 102:237–250.

Shmuel A, Augath M, Oeltermann A, Logothetis NK. 2006. Negative functional MRI response correlates with decreases in neuronal activity in monkey visual area V1. Nat Neurosci. 9: 569–577.

Slotnick SD, Thompson WL, Kosslyn SM. 2005. Visual mental imagery induces retinotopically organized activation of early visual areas. Cereb Cortex. 15:1570–1583.

Smirnakis SM, Brewer AA, Schmid MC, Tolias AS, Schuz A, Augath M, Inhoffen W, Wandell BA, Logothetis NK. 2005. Lack of long-term cortical reorganization after macaque retinal lesions. Nature. 435:300–307.

Somers DC, Dale AM, Seiffert AE, Tootell RB. 1999. Functional MRI reveals spatially specific attentional modulation in human primary visual cortex. Proc Natl Acad Sci USA. 96:1663–1668.

Sunness JS, Liu T, Yantis S. 2004. Retinotopic mapping of the visual cortex using functional magnetic resonance imaging in a patient with central scotomas from atrophic macular degeneration. Ophthalmology. 111:1595–1598.

Teo PC, Sapiro G, Wandell BA. 1997. Creating connected representations of cortical gray matter for functional MRI visualization. IEEE Trans Med Imaging. 16:852–863.

Wandell BA, Chial S, Backus BT. 2000. Visualization and measurement of the cortical surface. J Cogn Neurosci. 12:739–752.

Zeki S, Shipp S. 1988. The functional logic of cortical connections. Nature. 335:311–317.